JAERI-Research
2001-030

HIGH EFFICIENCY SECOND-HARMONIC GENERATION IN MULTI-PASS QUADRATURE ARRANGEMENT

May 2001

Hiromitsu KIRIYAMA, Fumihiko NAKANO and Koichi YAMAKAWA

日本原子力研究所
Japan Atomic Energy Research Institute

本レポートは，日本原子力研究所が不定期に公刊している研究報告書です。
入手の問合わせは，日本原子力研究所研究情報部研究情報課（〒319-1195　茨城県那珂郡東海村）あて，お申し越しください。なお，このほかに財団法人原子力弘済会資料センター（〒319-1195　茨城県那珂郡東海村日本原子力研究所内）で複写による実費頒布をおこなっております。

This report is issued irregularly.
Inquiries about availability of the reports should be addressed to Research Information Division, Department of Intellectual Resources, Japan Atomic Energy Research Institute, Tokai-mura, Naka-gun, Ibaraki-ken, 319-1195, Japan.

編集兼発行　　日本原子力研究所

High Efficiency Second-harmonic Generation in Multi-pass Quadrature Arrangement

Hiromitsu KIRIYAMA, Fumihiko NAKANO and Koichi YAMAKAWA

Advanced Photon Research Center

Kansai Research Establishment

Japan Atomic Energy Research Institute

Kizu-cho, Souraku-gun, Kyoto

(Received February 20, 2001)

We report on multi-pass quadrature frequency conversion of high-energy and high-average-power lasers with high conversion efficiency for pumping high peak power, ultrashort pulse Ti:sapphire laser amplifiers. Using a four-pass quadrature second harmonic scheme with $KTiOPO_4$ (KTP) crystals, we obtained an efficiency from a fundamental laser energy into a total second-harmonic laser energy in excess of 80 % of a commercial Q-Switched 1064-nm Nd:YAG laser at a low input fundamental laser intensity of 76 MW/cm^2. For higher power operation, we employed a two-pass quadrature scheme with $CsLiB_6O_{10}$ (CLBO) crystals. We obtained a total second-harmonic output pulse energy of 2.73 J from an input 1064-nm fundamental pulse energy of 3.27 J of a custom-built Q-switched 1064-nm Nd:YAG laser system at a fundamental laser intensity of 330 MW/cm^2 at 10 Hz, corresponding to energy conversion efficiency of 83 %. We discuss the details of the design and performance of this frequency conversion scheme in terms of output energy, conversion efficiency and scalability.

Keywords: Frequency Conversion, Quadrature Arrangement, Second-harmonic Generation (SHG), Neodymium:YAG Lasers, $KTiOPO_4$ (KTP) Crystal, $CsLiB_6O_{10}$ (CLBO) Crystal

多重パス矩象波長変換方式を用いた高効率第二高調波発生

日本原子力研究所関西研究所光量子科学研究センター
桐山　博光・中野　文彦・山川　考一

(2001 年 2 月 20 日受理)

極短パルス・超高ピーク出力チタンサファイアレーザーの効率向上のために、励起光源である Nd:YAG レーザーの第二高調波光を効率よく変換できる多重パス矩象波長変換方式を新たに考案した。非線形光学結晶に $KTiOPO_4$ (KTP)を用いた基礎実験において、76 MW/cm^2 の低い入射レーザー光強度に対して 80 %以上の高い変換効率を得た。また、非線形光学結晶に $CsLiB_6O_{10}$ (CLBO)を用いた高出力動作時において、3.27 J の入射 Nd:YAG レーザー光に対して 2.73 J の第二高調波光出力が繰り返し率 10 Hz で得られた。このときのエネルギー変換効率は 83 %に相当する。この波長変換方式の出力エネルギー特性、波長変換効率特性とそのスケール則に関して設計、並びに特性について議論する。

関西研究所：〒619-0215 京都府相楽郡木津町梅美台 8 － 1

Contents

目次

1. INTRODUCTION

Nearly four decades frequency conversion through nonlinear processes is widely used for extending the utility of existing lasers by using nonlinear optical materials [1]-[11]. Second-harmonic generation (SHG) for solid-state laser systems operating in the near-infrared region is of particular interest for applications such as medical equipment [12], material processing [13], light source for laser display [14] and as pumping light source for other laser systems [15]-[19]. In fact the SHG of the Nd:YAG lasers is very attractive pumping light source for Ti:sapphire chirped pulse amplification (CPA) systems [15]-[17], [20],[21]. In order to generate green outputs a commonly used frequency conversion process is SHG based on the use of nonlinear crystals to produce 532-nm radiation from a Nd:YAG laser system operating at 1064-nm [22], [23]. Conversion efficiencies of around 50 % for SHG are typically obtained. For example, a conversion efficiency of about 40 % for the SHG of a 1064-nm Nd:YAG laser by use of KD_2PO_4 (DKDP) crystal was reported by Kogan and Crow [24]. Conversion efficiencies of about 50 % were obtained for frequency doubling in $KTiOPO_4$ (KTP) crystal using a 1064-nm Nd:YAG laser by Driscoll *et al.* [25], Stolzenberger [26], and Bolt *et al.* [27]. SHG efficiencies in the range of 40-50 % were obtained for a 1064-nm Nd:YAG laser using LiB_3O_5 (LBO), β-BaB_2O_4 (BBO), DKDP crystals by Borsutzky *et al.* [28]. Recently a SHG conversion efficiency of above 50 % has been reported for a 1064-nm Nd:YAG laser using $CsLiB_6O_{10}$ (CLBO) crystal by Yap *et al.* [11]. An impressive SHG efficiency as high as 80 % for a 1064-nm Nd:YAG laser was also reported with the use of DKDP crystal with carefully optimized large-aperture fundamental beam of extremely high spatial quality by Linford *et al.* [29]. However, the conversion efficiencies of less specialized laser beams have not attained levels efficiencies of above 80 %. Furthermore, a very high input fundamental laser intensity of about 10 GW/cm^2 is required to achieve efficiencies of this level. When operating at these intensities, intensity-dependent breakdown of dielectric or bulk materials and self-focusing that degrade spatial pulse quality may occur. These effects typically occur at around an ~ 5 GW/cm^2 for pulses in the ns-range. For these reasons the efficient SHG with low fundamental laser intensity is essential to realize compact high peak power Ti:Sapphire CPA systems.

A quadrature frequency conversion scheme employing a pair of crystals was proposed to achieve high conversion efficiency by Eimerl in 1987 [30]. A schematic of quadrature scheme for SHG is shown in Fig. 1. The two crystals are oriented for type II interaction and positioned so that the optic axes of these crystals are mutually orthogonal. The scheme has two specific features for achieving high conversion efficiency. First, the input laser beam after the first crystal is also suitable for the second crystal, so that both crystals participate effectively in conversion. Second, the polarization of the second-

harmonic output beam generated in the first crystal is unsuitable for interaction in the second which prevents back-conversion of energy to fundamental in the second crystal. Therefore the quadrature scheme has undoubted advantages over the scheme wherein only one crystal is used such as a wide input intensity range over which conversion is high and a relatively high tolerance to small angular misalignments and input laser beam divergence. For example, by using this scheme, conversion efficiencies of 70-80 % for frequency doubling of a 1053-nm Nd:YLF oscillator followed by three Nd:phosphate glass laser amplifiers were reported with the use of two DKDP crystals at input fundamental laser intensity levels from about 200 MW/cm^2 to 6 GW/cm^2 [30].

In this paper we present an effective and simple multi-pass quadrature frequency conversion scheme by using polarization rotation for pumping a Ti:sapphire CPA system. In a four-pass quadrature scheme for frequency doubling of a commercial Q-switched 1064-nm Nd:YAG laser in $KTiOPO_4$ (KTP) crystals, we obtained a total second-harmonic conversion efficiency in excess of 80 % at a low input fundamental laser intensity of 76 MW/cm^2. With an input fundamental pulse energy of 607 mJ, 480 mJ of total SHG pulse energy was obtained at a repetition rate of 10 Hz. For higher power operation, in a two-pass quadrature scheme using $CsLiB_6O_{10}$ (CLBO) crystals for frequency doubling of a custom-buit Q-switched 1064-nm Nd:YAG laser system, we obtained 2.73 J of total second-harmonic output pulse energy from an input fundamental pulse energy of 3.27 J corresponding to a energy conversion efficiency of 83 %, with an input fundamental laser intensity of 330 MW/cm^2 at 10 Hz. The incorporation of quadrature and multi-pass feature in this scheme provides a frequency conversion performance superior to that of comparable lasers in its class. This scheme can be easily scaled up by increasing the size of the nonlinear crystals to accommodate larger input fundamental laser beam cross-section.

The remainder of this paper is organized as following. In Section II, we provide a theoretical model which simulates the high conversion efficiency in this scheme. Then in Section III, we describe an arrangement of multi-pass quadrature scheme and the pumping geometry of the Ti:sapphire amplifier. In Section IV, the results of SHG experiments obtained with this scheme using a commercial Q-switched 1064-nm Nd:YAG laser and KTP crystals are presented. Finally, in Section V, we describe the prospects for higher energy and higher average power operation with the use of a custom-built Q-switched 1064-nm Nd:YAG laser system and CLBO crystals and also present results obtained with this system and compare with the simulations described in Section II.

2. THEORY OF CONVERSION EFFICIENCY FOR SECOND-HARMONIC GENERATION

In order to gain a better understanding of the behavior of SHG conversion efficiency, we used a numerical model based on the coupled wave equations for SHG of a monochromatic plane wave. The derivation of these equations and solution are given in detail in the original paper of Armstrong et al. [31]. It is assumed that the beam may be considered to be locally plane over small regions, so that the plane wave solution for SHG may be used locally at each temporal and spatial point . Also, it is assumed that the second-harmonic power is zero at the entrance face of each crystal. In the case of the quadrature scheme, this condition may be achieved because the second-harmonic output beam generated in the first crystal not be allowed to participate in the conversion process in the second crystal. Additionally, it is assumed that a constant value may be assigned to the dephasing across the entire beam.

The coupled equations for SHG are given by [31],[32]

$$\frac{\partial E_2}{\partial z} = CE_1^{\,2} e^{i\Delta kz} \tag{1}$$

$$\frac{\partial E_1}{\partial z} = -CE_2 E_1^{\,*} e^{-i\Delta kz} \tag{2}$$

$$C = 5.46 d_{eff} / \lambda_1 (n_1 n_2 n_3) \tag{3}$$

where C is the nonlinear coupling constant proportional to the effective nonlinear coefficient of the crystal, Δ k is the wave vector mismatch between the input fundamental laser beam and second-harmonic output beam, d_{eff} is the effective nonlinear coefficient, λ_1 is the input fundamental laser wavelength and n_n are refractive indexes. The amplitudes are scaled as $|E_n|^2 \equiv I_n$, where I_n is the intensity. d_{eff} and λ_1 are in units of pm/V, and μm, respectively, then the units of C are $GW^{-1/2}$. The notation used here is identical to that found in [32].

The local conversion efficiency at a particular temporal and spatial location of the beam may be written as a function of the local drive η_0 and the dephasing δ [32]. The drive is the source term for the generation of the electric field at the second harmonic, and the dephasing is the phase mismatch between second-harmonic waves at the exit and entrance planes of the crystal. The conversion efficiency is given by [32]

$$\eta = \tanh^2[\frac{1}{2}\tanh^{-1}(sn[2\eta_0^{\frac{1}{2}},\ 1+\delta^2 / 4\eta_0])] \tag{4}$$

$$\eta_0 = C^2 I L^2 \tag{5}$$

$$\delta = \frac{1}{2}\Delta kL \tag{6}$$

where *sn* is an elliptic Jacobi function, I is the input fundamental laser intensity and L is the crystal length. The Δk is primarily due to beam divergence [32]. Therefore, the Δk can be calculated as

$$\Delta k = \beta_\theta \Delta\theta \tag{7}$$

where β_θ is the angular sensitivity and $\Delta\theta$ is the beam divergence of the input fundamental laser beam.

The familiar solution to the coupled equations for zero wave vector mismatch or no input fundamental laser depletion are special cases of the above solution. First, for zero wave vector mismatch, $\Delta k = 0$, $\delta = 0$, and $\eta_0 = 1$. The equation (4) becomes

$$\eta = \tanh^2(\eta_0^{\frac{1}{2}}) \tag{8}$$

When the depletion of the input fundamental laser is small, we have $\eta_0 < 1$, the equation (4) becomes

$$\eta = \eta_0(\sin\delta / \delta)^2 \tag{9}$$

In the case of the input fundamental laser fields that have temporally and spatially Gaussian profiles, the following equation is considered.

$$E_1(r,t) = E_0 \exp[-(t/t_0)^2 - (r/r_0)^2] \tag{10}$$

where t_0 is the pulse width and r_0 is the beam radius.

These equations allow us to estimate the harmonic conversion under ideal conditions and also to anticipate some potential problems such as a reversal of the power flow. With the equations, we calculate the performance for high energy and high average power operation, which are described in Section V.

3. MULTI-PASS QUADRATURE FREQUENCY CONVERSION SCHEME

The configuration of the multi-pass quadrature frequency conversion scheme is shown in Fig.2 [33]. The input laser beam is passed through a thin-film polarizer and then reflected to enter the nonlinear optical crystals in the quadrature scheme with the

dichroic mirror D_1, which is high-reflection coated at 1064-nm and anti-reflection coated at 532-nm. The $\lambda/2$ plate before nonlinear optical crystals is set so that the polarization of the input laser beam is rotated to the correct orientation for efficient interaction in the crystals. After passing through the quadrature scheme it is reflected back for a second pass through the two crystals by dichroic mirror D_2. The polarization of the input laser beam is rotated by 90 degrees after two passes through the $\lambda/4$ plate, and is therefore reflected by the thin-film polarizer towards a mirror, which is high-reflection coated at 1064-nm, because the beam was rotated to *s*-polarized. The mirror reflected the beam back for two more passes for a total of four passes through the quadrature scheme. In the two-pass scheme described in Section V the mirror is removed, and the beam dumped. The generated second-harmonic output beams were extracted through the dichroic mirrors D_1 and D_2. A dual output scheme was used to avoid back-conversion of the second-harmonic output beam.

This scheme is to pump a Ti:sapphire amplifier which is shown schematically in Fig.3. Because the polarization of the generated second-harmonic output beams is random, the output beams can be separated into two linear polarized beams (*p*-polarization and *s*-polarization) by the use of thin-film polarizers. The beams are then rotated by $\lambda/2$ plates for correct orientation to the Ti:sapphire amplifier crystal in order to obtain sufficient absorption. It should be noted that the energies of the second-harmonic outputs emitted through dichroic mirrors D_1 and D_2 ,respectively are not equal. Due to longitudinal pumping of the Ti:sapphire amplifier with small angles between the pump and the Ti:sapphire beams as shown in Fig.3, the Ti:sapphire laser beam is propagated parallel to the gain gradient, whereby each ray of the beam experiences the same integral gain and the whole beam is amplified uniformly. The dual outputs also enables the Ti:sapphire amplifier to be pumped from both sides of the Ti:sapphire crystal at high fluence level without optical damage to the faces of the crystal.

4. EXPERIMENTAL RESULTS AND DISCUSSION

The experimental setup for four-pass quadrature frequency conversion is shown in Fig.4. A commercial Q-switched 1064-nm Nd:YAG laser (Continuum, Powerlite 9010) was used as a laser source. The laser generated 15 ns (full width at half maximum (FWHM)) pulses of the fundamental laser radiation at a repetition rate of 10 Hz. The diameter of the laser beam was 8.5 mm at which the power density is decreased to $1/e^2$ of its peak value. In this experiment the KTP crystals were used as the nonlinear optical crystals because of their large nonlinear coefficient, low absorption between 500-nm and 1400-nm, large acceptance angle, broad spectral and temperature bandwidths, and high

damage threshold [20], [21], [34]. The size of each KTP crystal used in the experiment was 10 mm×10 mm×10 mm (Crystal Associates, gray-tracking-resistant KTP). They were anti-reflection coated on their input and output faces at both 532-nm and 1064-nm, respectively. The crystals were cut appropriately for type II doubling of 1064-nm laser radiation. The crystals were mounted on rotation stages for optimizing their angles with the input beam at ambient temperature. During operation for a set input beam power density, the crystal angles were fine tuned for maximizing second-harmonic output. The *p*-polarized input fundamental laser beam that was transmitted through the optical isolator was passed through the quadrature arrangement a total of four times and the second-harmonic output beams generated were extracted through the dichroic mirrors D_1 and D_2. The optical isolator provided sufficient isolation between the Q-switched Nd:YAG laser and the frequency conversion part. The pulse energies at 532-nm and 1064-nm, respectively, were measured by a calibrated power meter.

Figure 5 shows the total 532-nm second-harmonic output pulse energy for the dual second-harmonic output beams as a function of the input 1064-nm fundamental laser pulse energy. The energies of the second-harmonic outputs emitted through each dichroic mirror D_1 and D_2 are also indicated. There was no compensation for optical losses such as reflection, absorption and scattering of the crystals, and transmission losses of the dichroic mirrors D_1 and D_2. As can be seen in this figure a total maximum second-harmonic output pulse energy of 486 mJ was obtained with 607 mJ of input fundamental laser pulse energy at 10 Hz.

Figure 6 shows the second-harmonic conversion efficiencies defined as the green energy outputs divided by the fundamental energy input, as a function of the input 1064-nm fundamental laser intensity. As can be seen, a total maximum second-harmonic conversion efficiency of over 80 % was achieved with a low input laser intensity of 76 MW/cm^2. The intensity was calculated from the measured values of pulse duration, pulse energy, and beam diameter. The high efficiency of the present scheme enables effective use of energy and hardware. The low input laser intensity also enables the use of a smaller laser source and allows to operate the laser beam without intensity-dependent damage to the nonlinear crystals and optical components. Photochromic damage (gray-tracking) often occurs in KTP crystals during high power frequency conversion [35]-[37]. Though the gray-tracking threshold depends on the repetition rate of the laser and the crystal growth technique, laser damage thresholds ranging from about 100 MW/cm^2 have been reported [35]-[37]. Therefore, the low input laser intensity (< 100 MW/cm^2) is suitable to avoid gray-tracking problems of KTP crystals in this scheme.

5. PROSPECTS FOR HIGH ENERGY AND HIGH AVERAGE POWER OPERATION

Various nonlinear optical crystals have been developed for frequency doubling of 1064-nm Nd:YAG laser. Among these, KTP, LiB_3O_5 (LBO), ß-BaB_2O_4 (BBO) and KD_2PO_4 (DKDP) are most widely used [21]. Though the former three crystals, KTP, LBO and BBO have large effective nonlinear coefficients [20], [21], [25], [28], their small crystal sizes are not suitable for the SHG of high power lasers for which a large laser beam diameter is typical. The DKDP crystal can be grown to a large single crystal possessing high optical quality and has high laser-induced damage threshold [21]. DKDP is therefore, still widely used in most high power laser systems. The CLBO crystal is a recently discovered borate crystal [38]. The crystal can be grown to large sizes in a relatively short period. The CLBO crystal is transparent below 200 nm and therefore has been used for the generation of fourth and fifth harmonics of the Nd:YAG laser. However, the CLBO crystal also possesses some attractive properties for SHG of the 1064-nm Nd:YAG laser as compared with DKDP crystal. Table 1 lists the nonlinear parameters for SHG of the 1064-nm Nd:YAG laser in DKDP and CLBO [11], [21], [39]. As seen, DKDP has a large angular bandwidth compared to the CLBO crystal. However, CLBO has a large effective nonlinear coefficient and large temperature bandwidth. The CLBO crystal also exhibits a high laser-induced bulk damage threshold, as measured by a 1 ns 1064-nm Nd:YAG laser pulse. The spectral bandwidths and walk-off angles for the CLBO and DKDP crystals are rather similar. For high power and high repetition rate SHG, the small nonlinear coefficient and narrow temperature bandwidth limit the use of DKDP crystal. The small angular bandwidth does not limit the use of the CLBO crystal because the large cross-section of the crystal allows the use of a large beam, which minimizes the angular divergence of the beam.Further more the high effective nonlinear coefficient of CLBO enables a short crystal length to be used, which minimizes angular dephasing. Yap *et al.* demonstrated experimentally that the SHG performance of 1064-nm Nd:YAG laser using the CLBO crystal is superior to that using the DKDP crystal. These results indicate that the CLBO crystal is suitable for SHG of high power and high repetition rate Nd:YAG laser.

The experimental setup is shown in Fig. 7. The experiment was carried out by introducing a beam from a custom-built high power Q-switched 1064-nm Nd:YAG laser system, operated at a repetition rate of 10 Hz [40], [41]. This laser system has a single-pass master oscillator power amplifier (MOPA) architecture (Fig. 8). In the system a single-longitudinal-mode master oscillator generated pulses of about 13 ns duration and 180 mJ energy that were then shaped by a ~5.8 mm soft aperture to flat-top profile in space. The image of the soft aperture was relayed by means of a spatial filter which reduced the diffractive growth of spatial irradiance noise [42] through a pre-amplifier. The beam was then split into two parallel chains of larger size single-pass main-amplifiers. Gain isolation was provided by Pockels cells placed between the pre-amplifier and the

main-amplifier 1, and the main-amplifier 2 and main-amplifier 3. Faraday rotators were used to prevent pulses from propagating backward down the laser chain, placed between the oscillator and the pre-amplifier, the pre-amplifier and the main-amplifier 1, the main-amplifier 2 and the main-amplifier 3. The laser pulse from the oscillator was amplified in the pre-amplifier to ~700 mJ. The beam diameter after pre-amplifier was expanded to double its size to suit the larger diameter main-amplifier. The four main-amplifiers per chain were connected with each other by three image relay telescopes, which enabled them to propagate a laser beam with uniform intensity profile while avoiding damage to the optics. Also, compensation techniques using 90° quartz rotator were used to reduce thermal birefringence effects in the main-amplifiers. The laser pulse from the oscillator was amplified to ~7 J per chain with the four main-amplifiers whose performance per chain is summarized in Table II. The temporal profile of the beam from the system was observed to be smooth and near Gaussian, and the spatial profile near flat-top. For the present experiment we used one of the two main-amplifier chains in the system. The beam diameter was 10.9 mm at which the power density is decreased to $1/e^2$ of its peak value and the pulse duration about 13 ns (FWHM) in this experiment.

Each CLBO crystal (KOGAKUGIKEN Co., Ltd) had a cross section of 18 mm×18 mm and length of 10 mm and had no anti-reflection coatings. Each crystal was oriented for type II SHG of the input fundamental laser and was housed in a heater with a proportional-integral-derivative (PID) controller. The crystals were maintained constantly at 160 ℃ with an accuracy of 0.1 ℃ and were argon gas purged in order to avoid their degradation due to stresses introduced by crystal hydration, cutting, polishing, and thermal shock owing to laser power absorption [43]. The temperature-ramping rate was fixed at 2.3℃/min. The windows of the heaters were anti-reflection coated at both 1064-nm and 532-nm. Each heater was mounted on a rotation stage for optimizing the angle between the input beam and the crystal.

The *p*-polarized input fundamental laser beam was passed through an optical isolator which provided sufficient optical isolation between the high power Q-switched Nd:YAG laser and the frequency conversion part. As shown in Fig. 7, image relay telescopes were used to transport the input laser beam to the dichroic mirror D_2 after the CLBO crystals with a flat-top spatial profile while avoiding damage to the optics. The two CLBO crystals were placed in close proximity to each other at near the dichroic mirror D_2. The input laser beam was passed through the quadrature scheme a total of two times and the second-harmonic output beams generated were extracted through the dichroic mirrors D_1 and D_2. The pulse energies at 532-nm and 1064-nm, respectively, were measured by a calibrated power meter.

Figure 9 shows the total 532-nm second-harmonic output pulse energy for the dual second-harmonic output beams as a function of the input 1064-nm fundamental

laser pulse energy. The energies of the second-harmonic outputs emitted through each dichroic mirror D_1 and D_2 are also indicated. As mentioned before, there was no compensation for optical losses such as reflection, absorption and scattering of the crystals, and transmission losses of the dichroic mirrors D_1 and D_2. As seen from the figure, a total maximum second-harmonic output pulse energy of 2.73 J was obtained with 3.27 J of the input 1064-nm fundamental laser pulse energy at 10 Hz, corresponding to an average second-harmonic output power of 27.3 W. No power saturation was observed within the investigated power range.

Figure 10 shows the second-harmonic conversion efficiencies defined as the green energy outputs divided by the fundamental energy input, as a function of the input 1064-nm fundamental laser intensity. As can be seen in this figure, a total maximum second-harmonic conversion efficiency of 83 % was achieved with an input laser intensity of 330 MW/cm^2. As before, the intensity was calculated from the measured values of pulse duration, pulse energy, and beam diameter. The ability of CLBO crystals for efficient high power SHG of the Nd:YAG laser in a two-pass quadrature scheme was thus clearly demonstrated. The CLBO crystal has an extremely high damage threshold without the limitations such as gray-tracking.

In addition, the calculated conversion efficiency for a four-pass case was estimated to be 90 % based on the coupled equations described in Section II. Figure 11 shows the calculated performance for SHG of the 1064-nm Nd:YAG laser using CLBO crystals in a four-pass quadrature scheme together with the calculated and measured SHG conversion efficiencies in a two-pass quadrature scheme. The calculation assumed a beam divergence of 0.5 mrad and a pulse duration of 13 ns (FWHM). The profiles of time and space are assumed to be Gaussian and flat-top, respectively. The optical losses of the crystals and other optics such as reflection, transmission and Fresnel losses are also assumed. The effects due to beam walk-off and bulk absorption are small and therefore neglected. As shown in Fig. 11, the calculations for two-pass quadrature scheme are in good agreement with the experimental data which lends credibility to the possibility of achieving 90 % efficiency in the case of a four-pass quadrature scheme with an input fundamental laser intensity of about 500 MW/cm^2.

6. CONCLUSION

We have demonstrated efficient SHG of a 1064-nm Nd:YAG laser in a multi-pass quadrature scheme for pumping a high peak power, ultrashort pulse Ti:sapphire laser system. A conversion efficiency in excess of 80 % has been achieved with KTP at a low input fundamental laser intensity of 76 MW/cm^2 in a four-pass quadrature scheme. For an

input fundamental pulse energy of 607 mJ, 480 mJ of total SHG pulse energy was obtained at a repetition rate of 10 Hz. In a high power SHG experiment, a second-harmonic pulse energy of 2.73 J at 10 Hz was generated in CLBO with 83 % efficiency at an input fundamental laser intensity of 330 MW/cm^2 in a two-pass quadrature scheme. The large nonlinear coefficient and temperature bandwidth along with the large cross-section makes the CLBO crystal an excellent choice for efficient SHG of a high power and high repetition rate Nd:YAG laser. This scheme is currently being applied for pumping of a 40 mm diameter Ti:sapphire amplifier [15], [40],[41] in order to produce > 3 J of 800 nm radiation. The successful operation of this SHG scheme gives us the confidence that it is applicable and scalable to the design of high powered laser systems.

ACKNOWLEDGMENT

The authors would like to acknowledge A. Sagisaka, and Y. Akahane for their technical assistance. The authors would like to thank T. Arisawa, Y. Kato, and H. Ohno for their encouragement. One of the authors, H. Kiriyama, would like especially to express his gratitude to N. Srinivasan of Instruments Research and Development Establishment, Dhradun, India for helpful comments on the manuscript.

REFERENCES

[1] P. A. Franken, A. E. Hill, C. W. Peters, and G. Weinreich, "Genaration of optical harmonics," *Phys. Rev. Lett.*, vol. 7, pp. 118-119, Aug. 1961.

[2] J. A. Giordmaine, "Mixing of light beams in crystals," *Phys. Rev. Lett.*, vol. 8, pp. 19-20, Jan. 1962.

[3] R. C. Miller and A. Savage, "Harmonic generation and mixing of $CaWO_4$:Nd^{3+} and ruby pulsed laser beams in piezoelectric crystals," *Phys. Rev.*, vol. 128, pp. 2175-2179, Dec. 1962.

[4] F. Zernike, Jr., and P. R. Berman, "Generation of far infrared as a difference frequency," *Phys. Rev. Lett.*, vol. 15, pp. 999-1001, Dec. 1965.

[5] D. T. Attwood, E. L. Pierce and L. W. Coleman, "Converion efficiency and pulse shortening of a frequency-tripled, sub-nanosecond, 1.064 μm pulse," *Opt. Commun.*, vol. 15, pp. 10-12, Sep. 1975.

[6] D. T. Attwood, E. S. Bliss, E. L. Pierce and L. W. Coleman, "Laser frequency doubling in the presence of small-scale beam breakup," *IEEE J. Quantum Electron.*, vol. QE-12, pp. 203-204, Mar. 1977.

[7] R. M. Kogan, R. M. Pixton and T. G. Crow, "High-efficiency frequency doubling of Nd:YAG," *Opt. Eng.*, vol. 17, pp. 120-124, Mar.-Apr. 1978.

[8] O. I. Lavrovskaya, N. I. Pavlova, and A. V. Tarasov, "Second harmonic generation of light from an AlG:Nd^{3+} laser in an optically biaxial crystal of $KTiOPO_4$," *Sov. Phys. Crystallogr.*, vol. 31, pp. 678-681, Nov.-Dec. 1988.

[9] G. C. Bhar, S. Das, and P. K. Datta, "Efficient frequency doubling of Nd laser radiation," *Phys. Stat. Sol.*, vol. (a) 119, pp. K173-K176, 1990.

[10] J. Y. Huang, Y. R. Shen, C. Chen, and B. Wu, "Noncritically phase-matched second-harmonic generation and optical parametric amplification in a lithium triborate crystal," *Appl. Phys. Lett.*, vol. 58, pp. 1579-1581, Apr. 1991.

[11] Y. K. Yap, S. Haramura, A. Taguchi, Y. Mori, and T. Sasaki, "$CsLiB_6O_{10}$ crystal for frequency doubling the Nd:YAG laser," *Opt. Commun.*, vol. 145, pp. 101-104, Jan. 1998.

[12] M. V. Ortiz, D. J. Kuizenga, and J. H. Fair, "High average power second harmonic generation with $KTiOPO_4$," in *Advanced Solid-State Lasers OSA*, 1992, pp. 302-304.

[13] J. Golden, "Green lasers score good marks in semiconductor material processing," *Laser Focus World*, pp. 75-76, June 1992.

[14] T. V. Higgins, "Laser entertainment gets down to business at ILDA '91," *Laser Focus World*, pp. 15-16, Feb. 1992.

[15] K. Yamakawa, M. Aoyama, S. Matsuoka, H. Takuma, D. N. Fittinghoff, and C. P. J. Barty, "Ultrahigh-peak and high-average power chirped-pulse amplification of sub-20-fs pulses with Ti:sapphire amplifiers," *IEEE J. Select. Topics Quantum Electron.*, vol. 4, pp. 385-393, Mar.-Apr. 1998.

[16] Y. Nabekawa, Y. Kuramoto, T. Togashi, T. Sekikawa, and S. Watanabe, "Generation of 0.66 TW pulses at 1 kHz by a Tisapphire laser," *Opt. Lett.*, vol. 23, pp. 1384-1386, Sep. 1998.

[17] C. Rouyer, É. Mazataud, I. Allais, A. Pierre, S. Seznec, and C. Sauteret, "Generation of 50-TW femtosecond pulses in a Ti:sapphire/Nd:glass chain," *Opt. Lett.*, vol. 18, pp. 214-216, Feb. 1993.

[18] G. J. Hall and A. I. Ferguson, "LiB_3O_5 optical parametric oscillator pumped by a Q-switched frequency-doubled all-solid-state laser," *Opt. Lett.*, vol. 18, pp. 1511-1513, Sep. 1993.

[19] N. Srinivasan, H. Kiriyama, T. Kimura, M. Ohmi, M. Yamanaka, Y. Izawa, S. Nakai, and C. Yamanaka, "Efficient low energy near-infrared $KTiOPO_4$ optical parametric converter," *Opt. Lett.*, vol. 20, pp. 1265-1267, June 1995.

[20] J. D. Kmetec, J. J. Macklin, and J. F. Young, "0.5-TW, 125fs Ti:sapphire laser," *Opt. Lett.*, vol. 16, pp. 1001-1003, July 1991.

[21] C. P. J. Barty, C. L. Gordon III, and B. E. Lemoff, "Multiterawatt 30-fs Ti:sapphire

laser system," *Opt. Lett.*, vol. 19, pp. 1442-14444, Sep. 1994.

[22] W. Koechner, *Solid-State Laser Engineering*. Berlin, Germany: Springer, 1996.

[23] V. G. Dmitriev, G. G. Gurzadyan, and D. N. Nikogosyan, *Handbook of Nonlinear Optical Crystals*. Berlin, Germany: Springer, 1997.

[24] R. M. Kogan and T. G. Crow, "A high-brightness one Joule, frequency doubled Nd:YAG laser," *IEEE J. Quantum Electron.*, vol. QE-13, 1977.

[25] T. A. Driscoll, H. J. Hoffman, and R. E. Stone, "Efficient second-harmonic generation in KTP crystals," *J. Opt. Soc. Am. B*, vol. 3, pp. 683-686, May 1986.

[26] R. A. Stolzenberger, "Nonlinear optical properties of flux growth $KTiOPO_4$," *Appl. Opt.*, vol. 27, pp. 3883-3886, Sep. 1988.

[27] R. J. Bolt and M. van der Mooren, "Single shot bulk damage threshold and conversion efficiency measurements on flux grown $KTiOPO_4$ (KTP)," *Opt. Commun.*, vol. 100, pp. 399-410, July 1993.

[28] A. Borsutzky, R. Brünger, Ch. Huang, and R. Wallenstein, "Harmonic and sum-frequency generation of pulsed laser radiation in BBO, LBO, and KD*P," *Appl. Phys. B*, vol. 52, pp. 55-62, July 1991.

[29] G. J. Linford, B. L. Johnson, J. S. Hildum, W. E. Martin K. Sayder, R. D. Boyd, W. L. Smith, C. L. Vercimak, D. Eimerl, and J. J. Hunt, "Large aperture harmonic conversion experiments at Lawrence Livermore National Laboratory," *Appl. Opt.*, vol. 21, pp. 3633-3643, Oct. 1982.

[30] D. Eimerl, "Quadrature frequency conversion," *IEEE J. Quantum Electron.*, vol. QE-23, pp. 1361-1371, Aug. 1987.

[31] J. A. Armstrong, N. Bloembergen, J. Ducuing, and P. S. Pershan, "Interactions between light waves in a nonlinear dielectric," *Phys. Rev.*, vol. 127, pp. 1918-1939, Sep. 1962.

[32] D. Eimerl, "High average power harmonic generation," *IEEE J. Quantum Electron.*, vol. QE-23, pp. 575-592, May. 1987.

[33] H. Kiriyama, S. Matsuoka, Y. Maruyama, and T. Arisawa, "High efficiency second-harmonic generation in four-pass quadrature frequency conversion scheme," *Opt. Commun.*, vol. 174, pp. 499-502, Feb. 2000.

[34] F. C. Zumsteg, J. D. Bierlein, and T. E. Gier, "$K_xRb_{1-x}TiOPO_4$: A new nonlinear optical material," *J. Appl. Phys.*, vol. 47, pp. 4980-4985, Nov. 1976.

[35] J. C. Jacco, D. R. Rockafellow, and E. A. Teppo, "Bulk-darkening threshold of flux-grown $KTiOPO_4$," *Opt. Lett.*, vol. 16, pp. 1307-1309, Sep. 1991.

[36] B. Boulanger and M. M. Fejer, R. Blachman, and P. F. Bordui, "Study of $KTiOPO_4$ gray-tracking at 1064, 532, and 355 nm," *Appl. Phys. Lett.*, vol. 65, pp. 2401-2403, Nov. 1994.

[37] J. P. Fève, B. Boulanger, and G. Marnier, "Repetition rate dependency of gray-

tracking in $KTiOPO_4$ during second-harmonic generation at 532 nm," *Appl. Phys. Lett.*, vol. 70, pp. 277-279, Jan. 1997.

[38] Y. Mori, I. Kuroda, S. Nakajima, T. Sasaki, and S. Nakai, "New nonlinear optical crystals: Cesium lithium borate," *Appl. Phys. Lett.*, vol. 67, pp. 1818-1820, Sep. 1995.

[39] Y. Mori and T. Sasaki, "$CsLiB_6O_{10}$ crystal: Growth and Properties," *Proc. SPIE*, vol. 2700, pp. 20-27, 1996.

[40] K. Yamakawa, M. Aoyama, S. Matsuoka, T. Kase, Y. Akahane, and H. Takuma, "100-TW sub-20fs Ti:sapphire laser system operating at a 10-Hz repetition rate," *Opt. Lett.*, vol. 23, pp. 1468-1470, Sep. 1998.

[41] K. Yamakawa and C.P. J. Barty, "Ultrafast, ultrahigh-peak, and high-average power Ti:sapphire laser system and its applications," *IEEE J. Select. Topics Quantum Electron.*, vol. 6, pp. 658-675, July-Aug. 2000.

[42] W. W. Simmons, J. T. Hunt, and W. E. Warren, "Light propagation through large laser systems," *IEEE J. Quantum Electron.*, vol. QE-17, pp. 1727-1744, Sep. 1981.

[43] Y. K. Yap, T. Inoue, H. Sakai, Y. Kagebayashi, Y. Mori, T. Sasaki, K. Deki, and M. Horiguchi, "Long-term operation of $CsLiB_6O_{10}$ at elevated crystal temperature," *Opt. Lett.*, vol. 23, pp. 34-36, Jan. 1998.

crystal (type II)	phase-matching angle [degree]	effective nonlinear coefficient [pm/V]	angular bandwidth [mrad-cm]	spectral bandwidth [nm-cm]	temperature bandwidth [degree-cm]	walk-off angle [degree]	damage threshold [GW/cm^2]
DKDP	53.5	0.40	5.0	5.57	6.7	1.38	6
CLBO	41.9	0.95	1.7	5.60	43.1	1.78	26

TABLE 1 NONLINEAR PARAMETERS FOR SHG OF THE 1064-nm Nd:YAG LASER IN DKDP AND CLBO [2], [8], [17]

stage	rod size	lamp input energy [J]	output energy [J]
oscillator	6 mmϕ ×115 mml	18	0.18
pre-amplifier	6 mmϕ ×115 mml	18	0.70 (before split)
main-amplifier 1	12 mmϕ ×115 mml	77	1
main-amplifier 2	12 mmϕ ×115 mml	77	3
main-amplifier 3	12 mmϕ ×115 mml	77	5
main-amplifier 4	12 mmϕ ×115 mml	77	7

TABLE 2 PERFORMANCE SUMMARY OF CUSTOM-BUILT HIGH POWER Q-SWITCHED 1064-nm Nd:YAG LASER SYSTEM

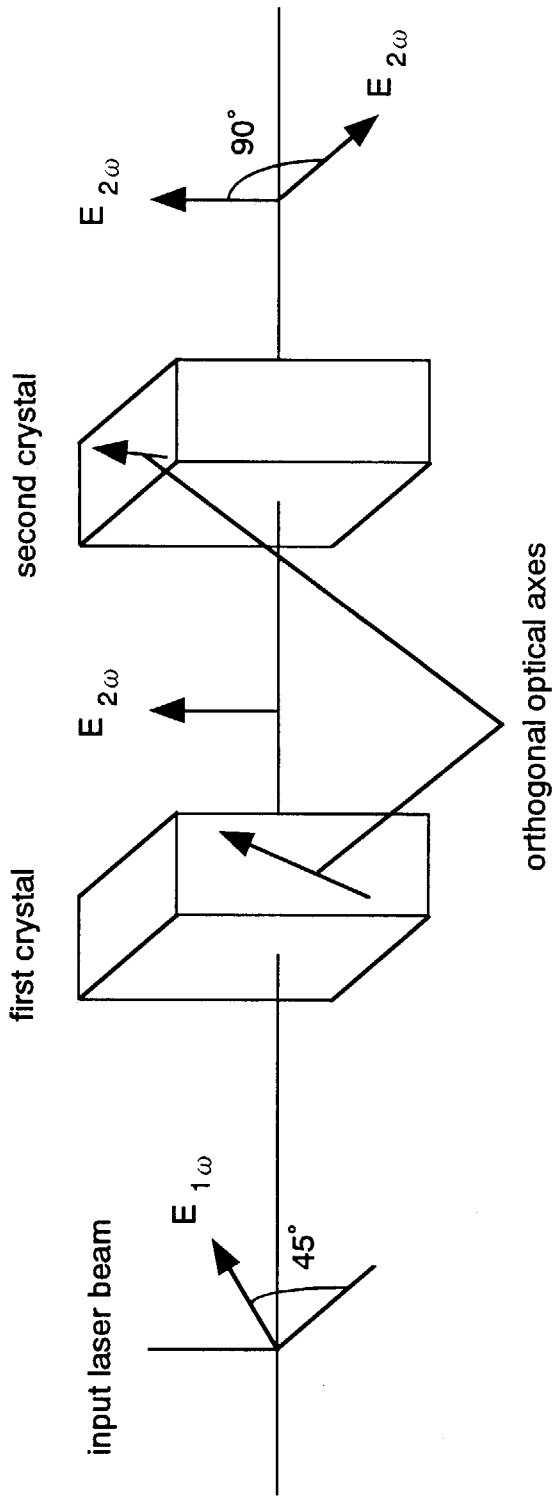

Fig.1 Type II quadrature frequency conversion scheme used for SHG.

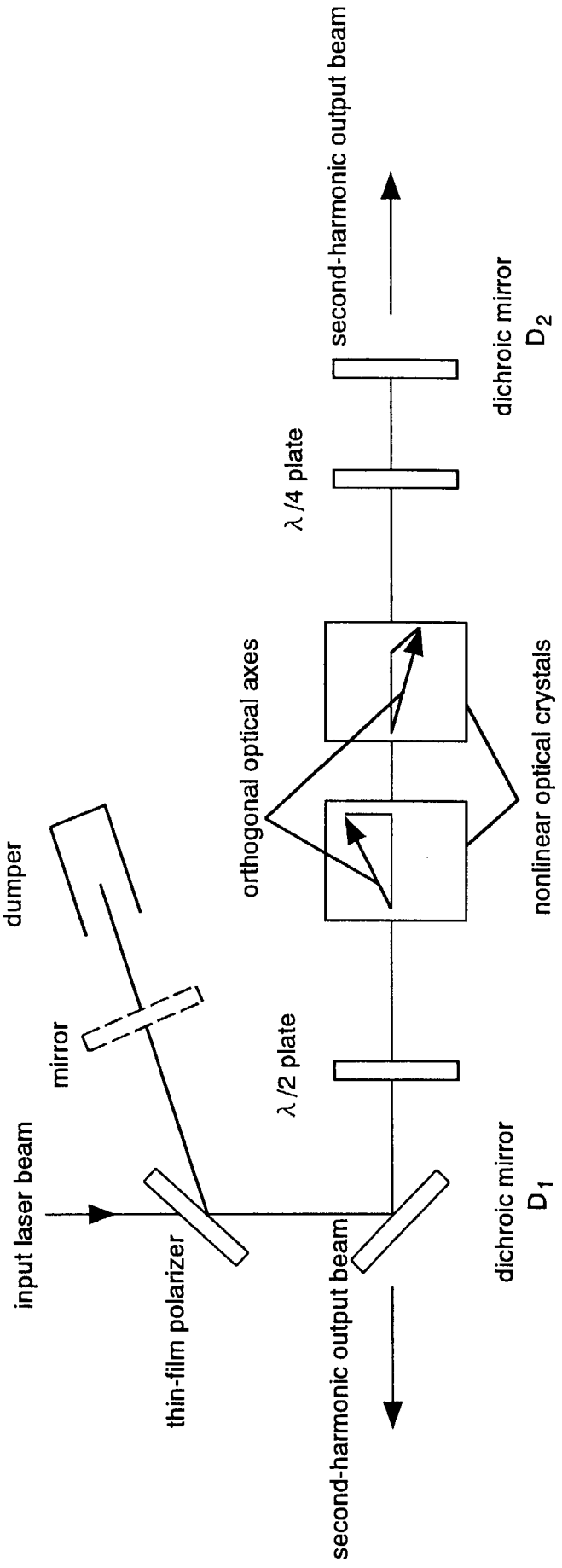

Fig.2 Configuration of a four-pass quadrature frequency conversion scheme. Mirror is removed for a two-pass case.

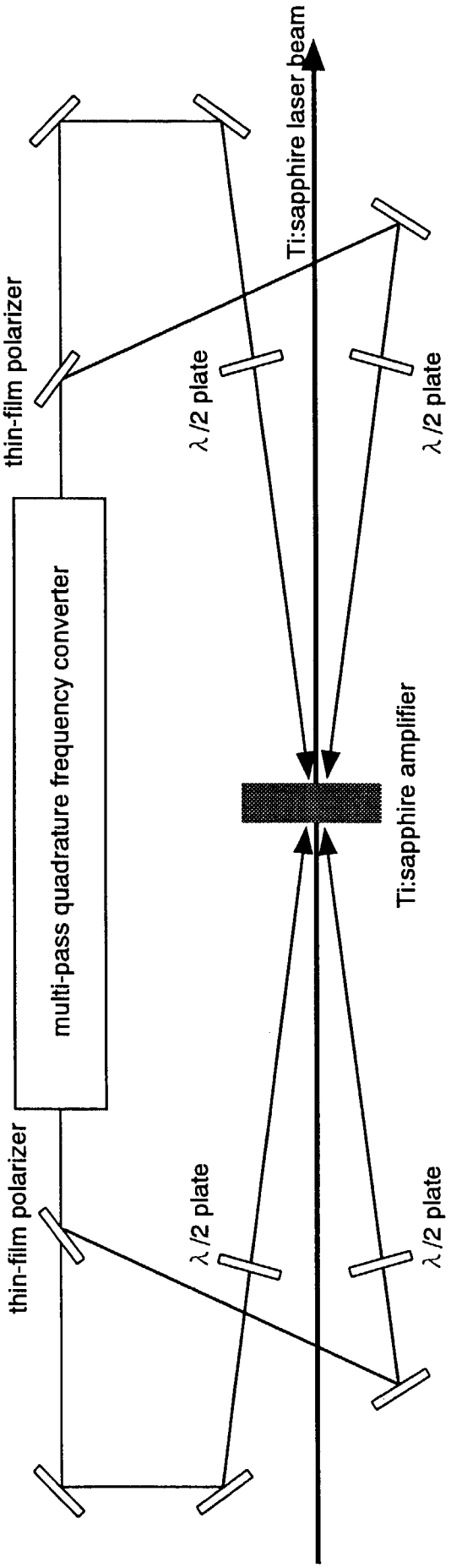

Fig.3 Schematic diagram of pumping a Ti:sapphire amplifier.

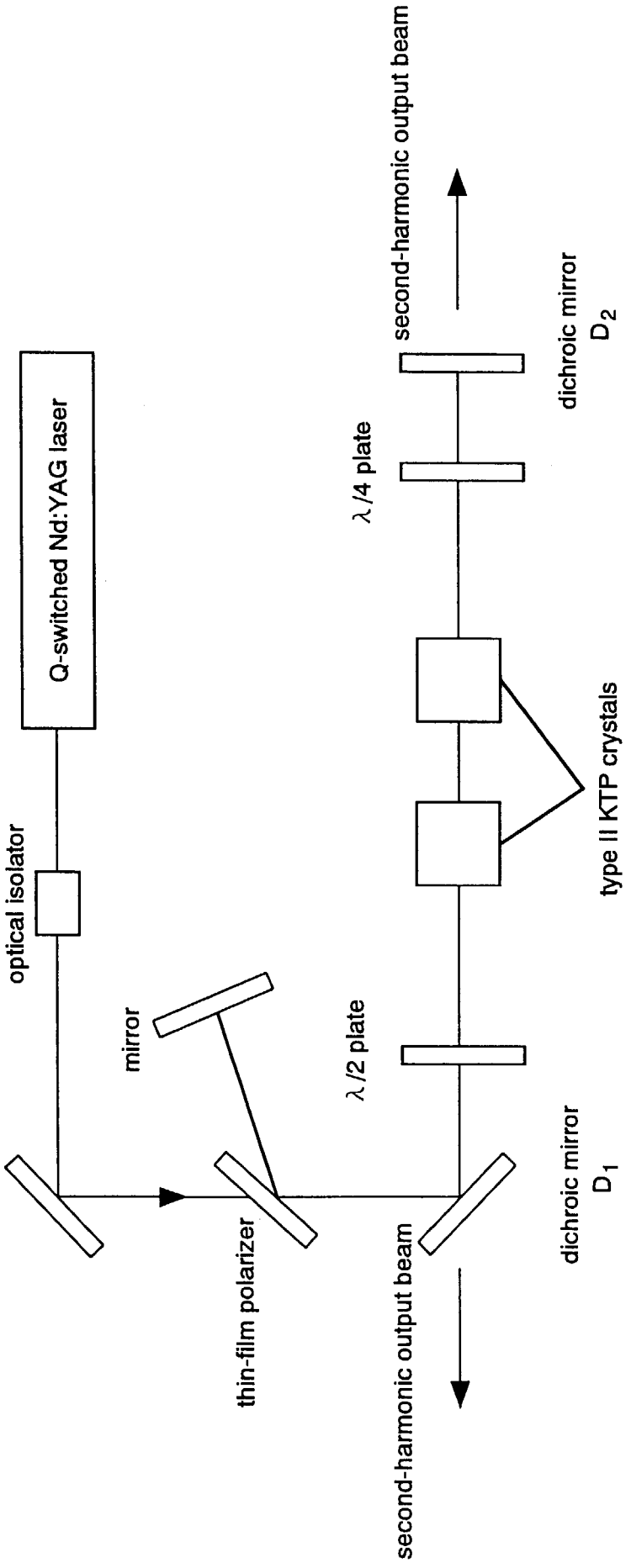

Fig.4 Experimental setup for SHG in a four-pass quadrature scheme using KTP crystals.

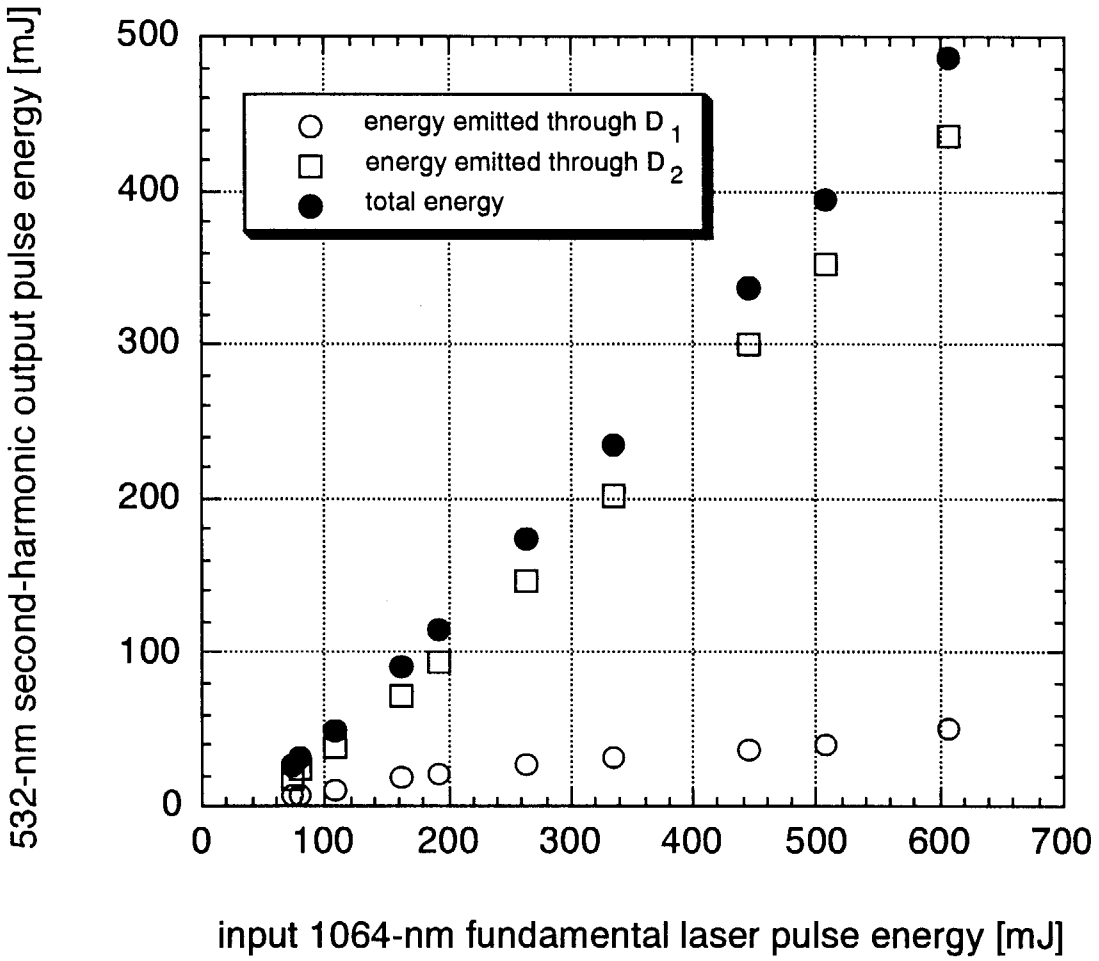

Fig.5 total 532-nm second-harmonic output energy emitted through both dichroic mirrors D_1 and D_2 versus the input 1064-nm fundamental laser energy in a four-pass scheme using KTP crystals. The energy emitted through each dichroic mirror D_1 and D_2 are also shown.

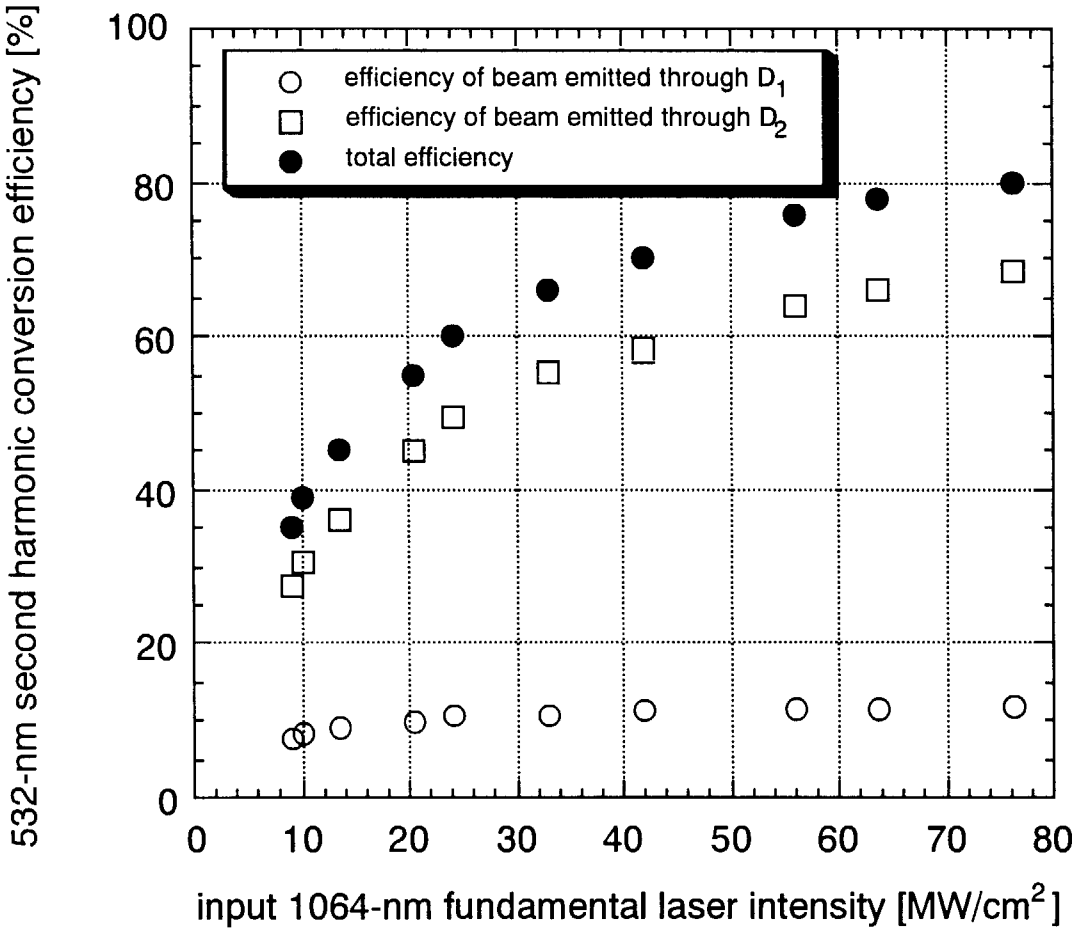

Fig.6 total 532-nm second-harmonic conversion efficiency of beams emitted through both dichroic mirrors D_1 and D_2 versus the input 1064-nm fundamental laser intensity in a four-pass quadrature scheme using KTP crystals. The efficiency of beam emitted through each dichroic mirror D_1 and D_2 are also shown.

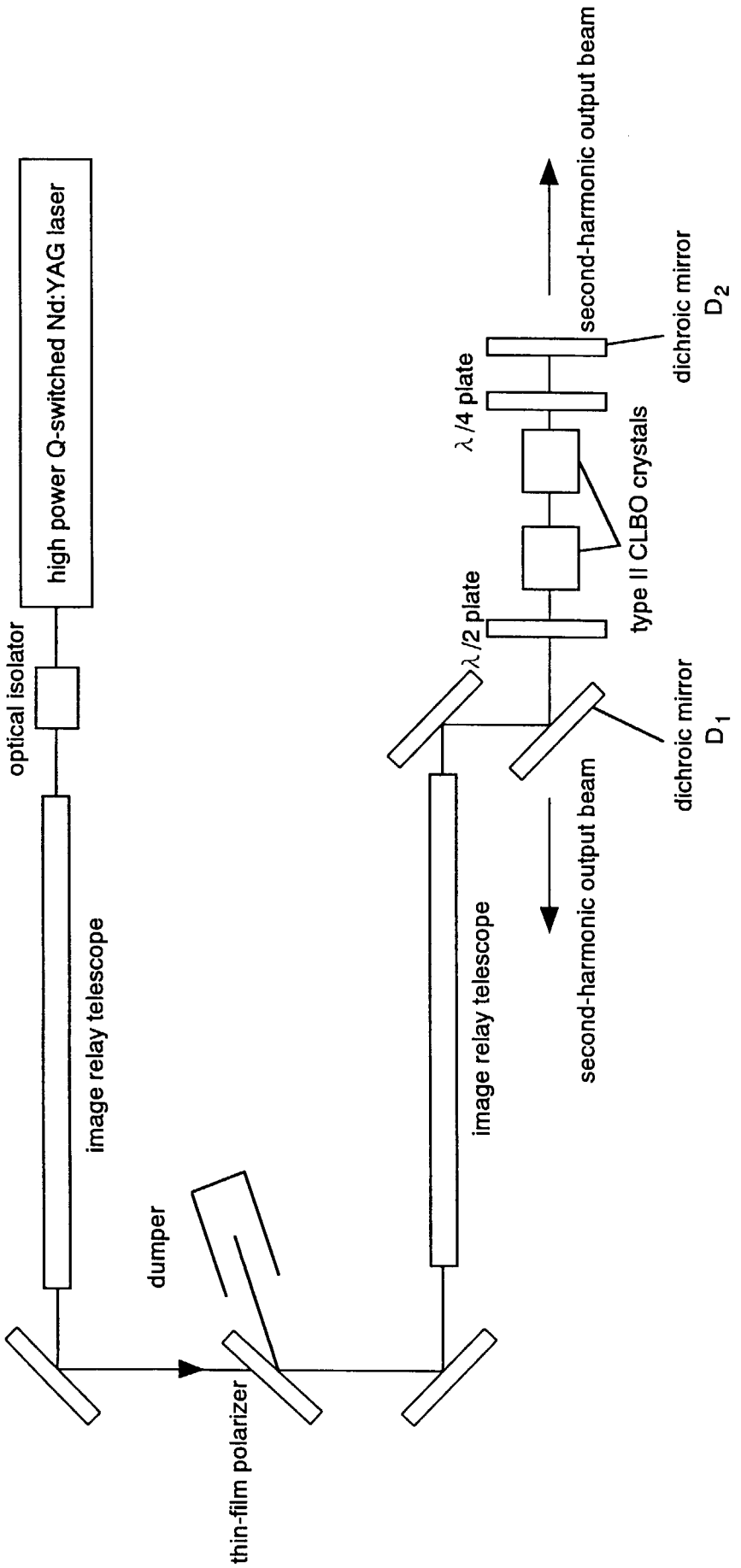

Fig.7 Experimental setup for SHG in a two-pass quadrature scheme using CLBO crystals.

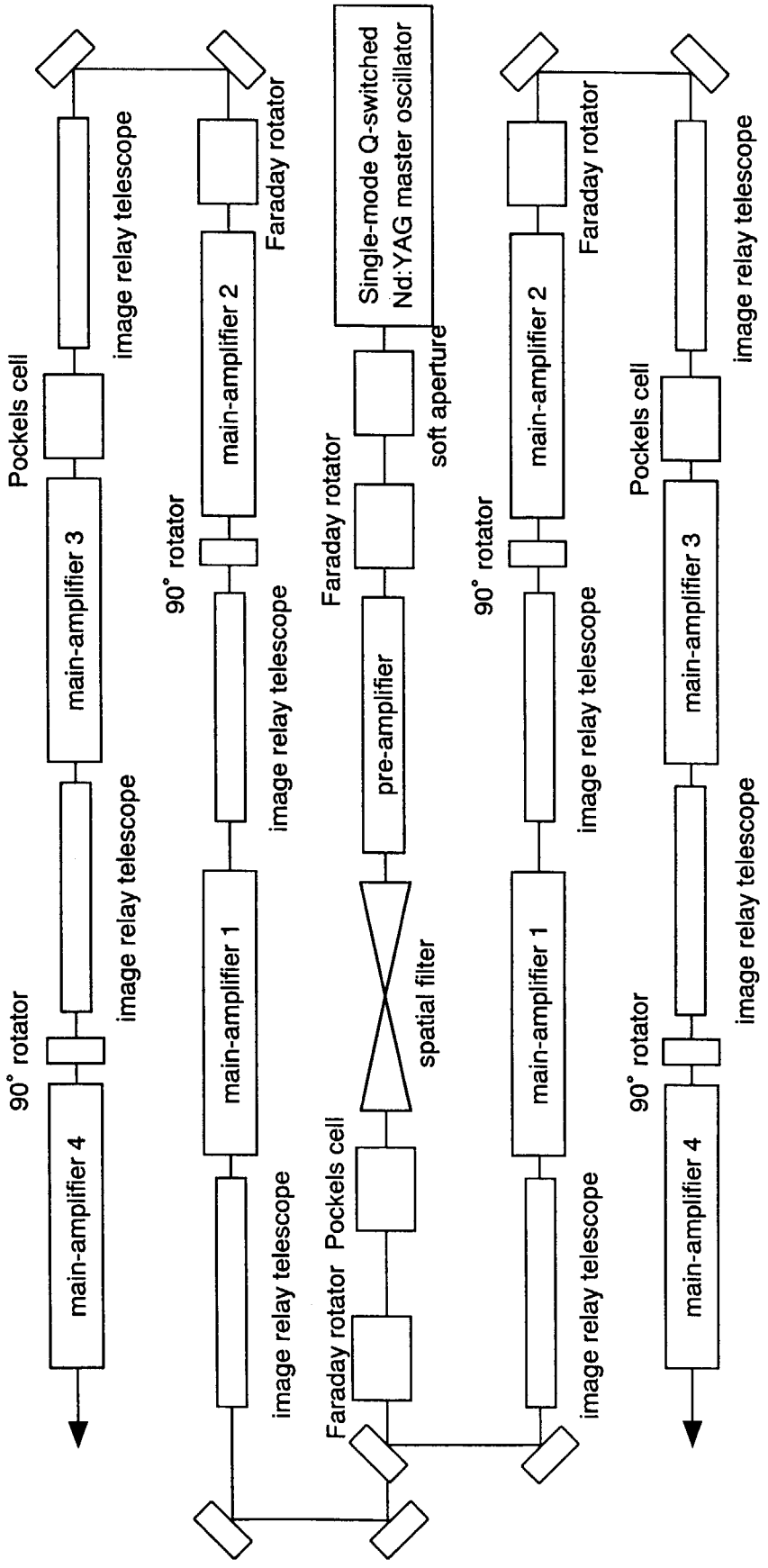

Fig.8 layout of the custom-built high power Q-switched 1064-nm Nd:YAG laser system.

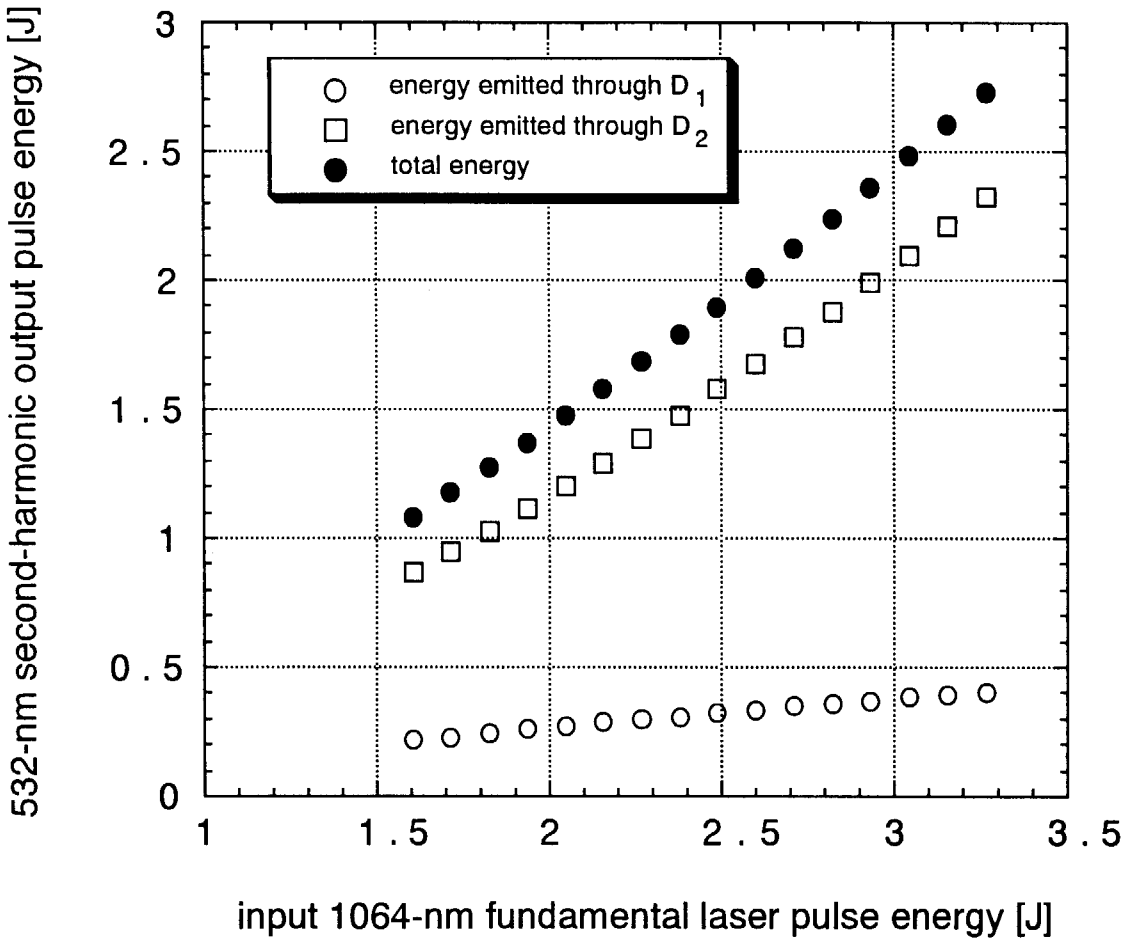

Fig.9 total 532-nm second-harmonic output energy emitted through both dichroic mirrors D_1 and D_2 versus the input 1064-nm fundamental laser energy in a two-pass quadrature scheme using CLBO crystals. The energy emitted through each dichroic mirror D_1 and D_2 are also shown.

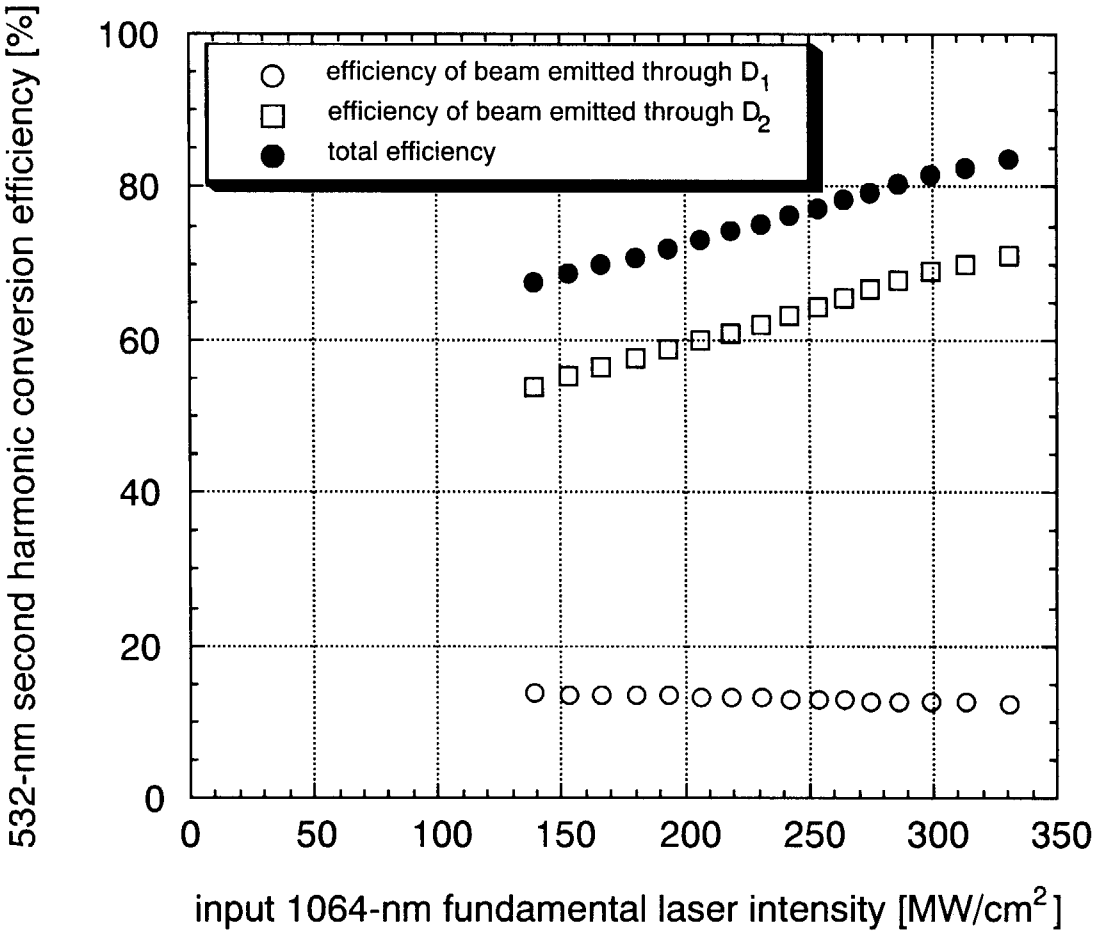

Fig.10 total 532-nm second-harmonic conversion efficiency of beams emitted through both dichroic mirrors D_1 and D_2 versus the input 1064-nm fundamental laser intensity in a two-pass quadrature scheme using CLBO crystals. The efficiency of beam emitted through each dichroic mirror D_1 and D_2 are also shown.

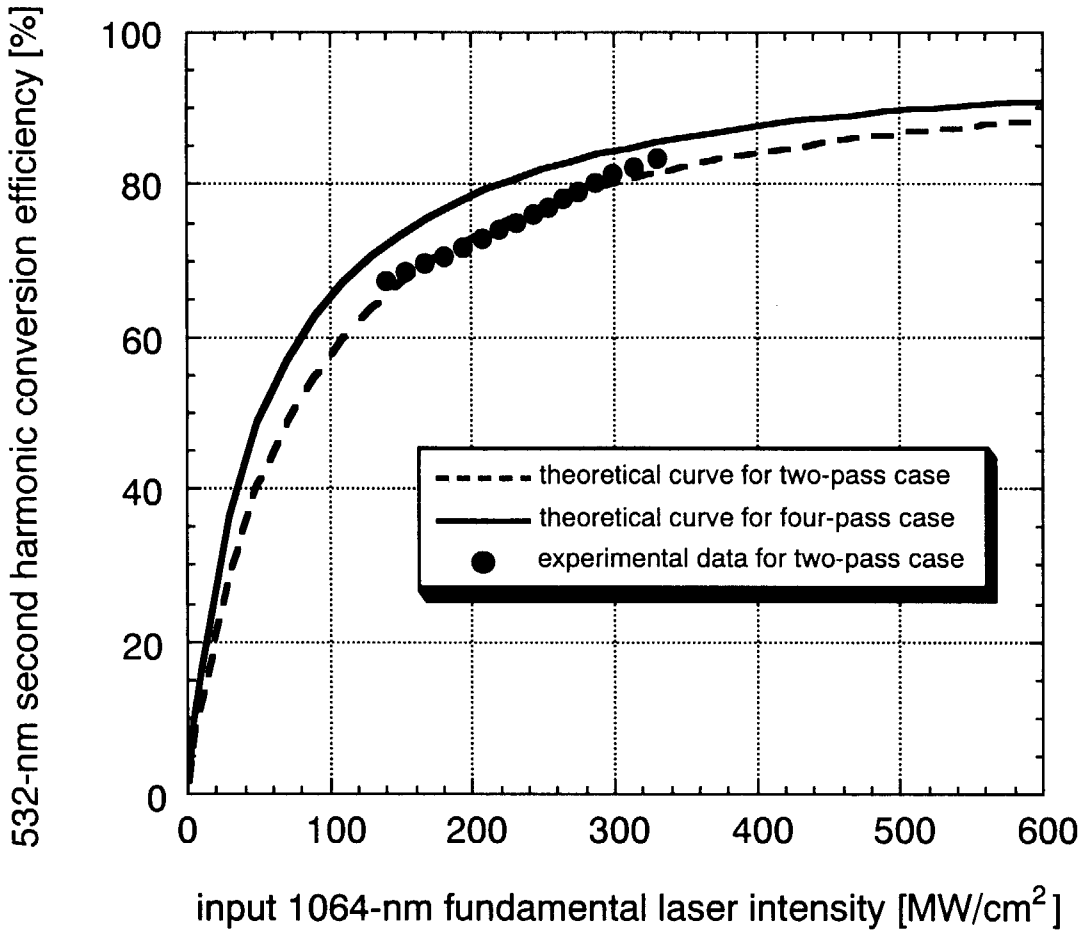

Fig.11 Calculated conversion efficiencies for SHG of the 1064-nm Nd:YAG laser using CLBO crystals in a four-pass quadrature scheme with the calculated and measured SHG conversion efficiencies in a two-pass quadrature scheme.

国際単位系（SI）と換算表

表1　SI基本単位および補助単位

量	名称	記号
長さ	メートル	m
質量	キログラム	kg
時間	秒	s
電流	アンペア	A
熱力学温度	ケルビン	K
物質量	モル	mol
光度	カンデラ	cd
平面角	ラジアン	rad
立体角	ステラジアン	sr

表2　SIと併用される単位

名称	記号
分，時，日	min, h, d
度，分，秒	°, ′, ″
リットル	l, L
トン	t
電子ボルト	eV
原子質量単位	u

1 eV=1.60218×10^{-19}J

1 u=1.66054×10^{-27}kg

表3　固有の名称をもつSI組立単位

量	名称	記号	他のSI単位による表現
周波数	ヘルツ	Hz	s^{-1}
力	ニュートン	N	$m\cdot kg/s^2$
圧力，応力	パスカル	Pa	N/m^2
エネルギー,仕事,熱量	ジュール	J	N·m
工率，放射束	ワット	W	J/s
電気量，電荷	クーロン	C	A·s
電位，電圧，起電力	ボルト	V	W/A
静電容量	ファラド	F	C/V
電気抵抗	オーム	Ω	V/A
コンダクタンス	ジーメンス	S	A/V
磁束	ウェーバ	Wb	V·s
磁束密度	テスラ	T	Wb/m^2
インダクタンス	ヘンリー	H	Wb/A
セルシウス温度	セルシウス度	℃	
光束	ルーメン	lm	cd·sr
照度	ルクス	lx	lm/m^2
放射能	ベクレル	Bq	s^{-1}
吸収線量	グレイ	Gy	J/kg
線量等量	シーベルト	Sv	J/kg

表4　SIと共に暫定的に維持される単位

名称	記号
オングストローム	Å
バーン	b
バール	bar
ガル	Gal
キュリー	Ci
レントゲン	R
ラド	rad
レム	rem

1 Å=0.1nm=10^{-10}m

1 b=100fm^2=10^{-28}m^2

1 bar=0.1MPa=10^{5}Pa

1 Gal=1cm/s^2=10^{-2}m/s^2

1 Ci=3.7×10^{10}Bq

1 R=2.58×10^{-4}C/kg

1 rad=1cGy=10^{-2}Gy

1 rem=1cSv=10^{-2}Sv

表5　SI接頭語

倍数	接頭語	記号
10^{18}	エクサ	E
10^{15}	ペタ	P
10^{12}	テラ	T
10^{9}	ギガ	G
10^{6}	メガ	M
10^{3}	キロ	k
10^{2}	ヘクト	h
10^{1}	デカ	da
10^{-1}	デシ	d
10^{-2}	センチ	c
10^{-3}	ミリ	m
10^{-6}	マイクロ	μ
10^{-9}	ナノ	n
10^{-12}	ピコ	p
10^{-15}	フェムト	f
10^{-18}	アト	a

（注）

1．表1－5は「国際単位系」第5版，国際度量衡局1985年刊行による。ただし，1 eVおよび1 uの値はCODATAの1986年推奨値によった。

2．表4には海里，ノット，アール，ヘクタールも含まれているが日常の単位なのでここでは省略した。

3．barは，JISでは流体の圧力を表わす場合に限り表2のカテゴリーに分類されている。

4．EC閣僚理事会指令ではbar，barnおよび「血圧の単位」mmHgを表2のカテゴリーに入れている。

換算表

力	N(=10^{5}dyn)	kgf	lbf
	1	0.101972	0.224809
	9.80665	1	2.20462
	4.44822	0.453592	1

粘度　1 Pa·s(N·s/m^2)=10 P(ポアズ)(g/(cm·s))

動粘度　1m^2/s=10^{4}St(ストークス)(cm^2/s)

圧力	MPa(=10bar)	kgf/cm^2	atm	mmHg(Torr)	lbf/in^2(psi)
	1	10.1972	9.86923	7.50062×10^3	145.038
	0.0980665	1	0.967841	735.559	14.2233
	0.101325	1.03323	1	760	14.6959
	1.33322×10^{-4}	1.35951×10^{-3}	1.31579×10^{-3}	1	1.93368×10^{-2}
	6.89476×10^{-3}	7.03070×10^{-2}	6.80460×10^{-2}	51.7149	1

エネルギー・仕事・熱量	J(=10^7 erg)	kgf·m	kW·h	cal(計量法)	Btu	ft·lbf	eV
	1	0.101972	2.77778×10^{-7}	0.238889	9.47813×10^{-4}	0.737562	6.24150×10^{18}
	9.80665	1	2.72407×10^{-6}	2.34270	9.29487×10^{-3}	7.23301	6.12082×10^{19}
	3.6×10^6	3.67098×10^5	1	8.59999×10^5	3412.13	2.65522×10^6	2.24694×10^{25}
	4.18605	0.426858	1.16279×10^{-6}	1	3.96759×10^{-3}	3.08747	2.61272×10^{19}
	1055.06	107.586	2.93072×10^{-4}	252.042	1	778.172	6.58515×10^{21}
	1.35582	0.138255	3.76616×10^{-7}	0.323890	1.28506×10^{-3}	1	8.46233×10^{18}
	1.60218×10^{-19}	1.63377×10^{-20}	4.45050×10^{-26}	3.82743×10^{-20}	1.51857×10^{-22}	1.18171×10^{-19}	1

1 cal= 4.18605J（計量法）

= 4.184J（熱化学）

= 4.1855J（15 C）

= 4.1868J（国際蒸気表）

仕事率　1 PS(仏馬力)

= 75 kgf·m/s

= 735.499W

放射能	Bq	Ci
	1	2.70270×10^{-11}
	3.7×10^{10}	1

吸収線量	Gy	rad
	1	100
	0.01	1

照射線量	C/kg	R
	1	3876
	2.58×10^{-4}	1

線量当量	Sv	rem
	1	100
	0.01	1

（86年12月26日現在）

High Efficiency Second-Harmonic Generation in Multi-Pass Quadrature Arrangement